



Insertion of nitrene and chalcogenolate groups into the Ir–C σ bond in a cyclometalated iridium(III) complex

Yiu-Keung Sau, Xiao-Yi Yi, Ka-Wang Chan, Chun-Sing Lai, Ian D. Williams, Wa-Hung Leung*

Department of Chemistry, The Hong Kong University of Science and Technology, Clear Water Bay, Kowloon, Hong Kong, PR China

ARTICLE INFO

Article history:

Received 5 January 2010
Received in revised form 2 February 2010
Accepted 2 February 2010
Available online 10 February 2010

Keywords:

Iridium
Cyclometalated
Insertion
Nitrene

ABSTRACT

Treatment of $[\text{Cp}^*\text{Ir}(\text{ppy})\text{Cl}]$ ($\text{Cp}^* = \eta^5\text{-C}_5\text{Me}_5$, $\text{ppyH} = 2\text{-}(2\text{-pyridyl})\text{phenyl}$) with $\text{Ag}(\text{OTf})$ ($\text{OTf}^- = \text{triflate}$) in MeOH and MeCN gave the solvento complexes $[\text{Cp}^*\text{Ir}(\text{ppy})(\text{solv})][\text{OTf}]$ ($\text{solv} = \text{MeOH}$ (**1**) and MeCN (**2**)). Complex **1** is capable of catalyzing oxidation and aziridination of styrene with PhIO and PhINTs (Ts = tosyl), respectively. Treatment of **2** with a stoichiometric amount of PhINTs resulted in the insertion of the NTs group into the Ir–C(ppy) bond and formation of $[\text{Cp}^*\text{Ir}(\eta^2\text{-ppy-NTs})(\text{MeCN})][\text{OTf}]$ (**3**). Treatment of **1** with R_2E_2 afforded $[\text{Cp}^*\text{Ir}(\text{ppy})(\eta^1\text{-R}_2\text{E}_2)][\text{OTf}]$ ($\text{E} = \text{S}$ (**4**), Se (**5**), Te (**6**)). Reactions of **4** and **5** with $\text{Ag}(\text{OTf})$ resulted in cleavage of the E–E bond and insertion of an ER group into the Ir–C(ppy) bond. The crystal structures of complexes **2–6** and $[\text{Cp}^*\text{Ir}(\eta^2\text{-ppy-S-}i\text{-}p\text{-tol})(\text{H}_2\text{O})][\text{OTf}]_2$ have been determined.

© 2010 Elsevier B.V. All rights reserved.

1. Introduction

Half-sandwich iridium cyclopentadienyl complexes have received considerable attention due to their applications in C–H activation and functionalization [1–3]. Of note is cationic $[\text{Cp}^*\text{Ir}(\text{PMe}_3)\text{Me}(\text{solv})]^+$ ($\text{Cp}^* = \eta^5\text{-C}_5\text{Me}_5$) that can activate alkane C–H bonds under mild conditions [3]. One possible mechanism for the $\text{Cp}^*\text{Ir}(\text{III})$ -mediated C–H activation involves an oxidative addition–reductive elimination pathway [3–7]. Therefore, in order to develop efficient Ir-based catalysts for C–H activation, knowledge of the organometallic chemistry of higher valent Cp^*Ir complexes is essential.

In an attempt to synthesize high-valent Ir complexes, we sought to investigate the oxidation reactions of Cp^*Ir complexes stabilized by bidentate, cyclometalated 2-(2-pyridyl)phenyl (ppy) ligands. Our interest in high valent cyclometalated iridium complexes is stimulated by recent reports that Ir–ppy complexes are capable of catalyzing oxidation of water using Ce^{IV} as the primary oxidant [8,9]. A theoretical study showed that the electronic structure of an electrophilic Ir–oxo species, namely $[\text{Cp}^*\text{Ir}(\text{O})(\text{ppy})]^+$, is consistent with this complex being the reactive intermediate for the Ir-mediated water oxidation [8]. High-valent Ir complexes containing metal–ligand multiple bonds are rare. The only structurally characterized Ir terminal oxo complex is tetrahedral $[\text{Ir}^{\text{V}}(\text{O})(\text{mes})_3]$ (mes = mesityl) [10]. The Ir^{III} complexes $[\text{Cp}^*\text{Ir}(\text{NR})]$ [11], $[\text{Cp}^*_2\text{Ir}_2(\mu\text{-O})_2(\text{PPh}_3)]$ [12] and $[\text{Cp}^*_2\text{Ir}_2(\mu\text{-NBu}^t)(\mu\text{-O})]$ [13] have been isolated by Bergman and coworkers. Nevertheless, $\text{Cp}^*\text{Ir}^{\text{V}}$

complexes with terminal oxo and imido ligands are unknown. This prompted us to explore the atom transfer chemistry of $\text{Cp}^*\text{Ir}(\text{ppy})$ complexes. In this work, we describe the reactions of $[\text{Cp}^*\text{Ir}(\text{ppy})(\text{solv})]^+$ with oxo and nitrene donors. We found that reaction of $[\text{Cp}^*\text{Ir}(\text{ppy})(\text{MeCN})]^+$ with PhINTs (Ts = tosyl) resulted in insertion of the nitrene group into the Ir–C(ppy) bond. Also, the treatment of $\text{Cp}^*\text{Ir}(\text{ppy})(\eta^1\text{-R}_2\text{E}_2)$ ($\text{E} = \text{S}$, Se) with Ag^{I} led to E–E cleavage and insertion of an ER group into the Ir–C(ppy) bond. The crystal structures of $[\text{Cp}^*\text{Ir}(\eta^2\text{-ppy-NTs})(\text{MeCN})][\text{OTf}]$ and $[\text{Cp}^*\text{Ir}(\eta^2\text{-ppy-S-}i\text{-}p\text{-tol})(\text{H}_2\text{O})][\text{OTf}]_2$ will be reported.

2. Experimental

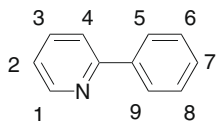
2.1. General

All manipulations were carried out under nitrogen by standard Schlenk techniques. Solvents were purified, distilled and degassed prior to use. NMR spectra were recorded on a Varian Mercury 300 spectrometer operating at 300 and 282.4 MHz for ^1H and ^{19}F , respectively. Chemical shifts (δ , ppm) were reported with reference to SiMe_4 (^1H and ^{13}C) and $\text{C}_6\text{H}_5\text{CF}_3$ (^{19}F). Elemental analyses were performed by Medac Ltd., Surrey, UK. The compound $[\text{Cp}^*\text{Ir}(\text{ppy})\text{Cl}]$ was synthesized as described elsewhere [14]. Atom labeling schemes for the ppyH ligand is shown in Scheme 1.

2.2. Preparation of $[\text{Cp}^*\text{Ir}(\text{ppy})(\text{H}_2\text{O})][\text{OTf}]$ (**1**)

To a suspension of $[\text{Cp}^*\text{Ir}(\text{ppy})\text{Cl}]$ (50 mg, 0.096 mmol) in methanol (10 mL) was added AgOTf (25 mg, 0.097 mmol). The color of

* Corresponding author. Tel.: +852 2358 7360; fax: +852 2358 1594.
E-mail address: chleung@ust.hk (W.-H. Leung).



Scheme 1. Atom labeling scheme for the ppyH ligand.

the mixture changed from orange to yellow and a white precipitate was formed. The mixture was stirred at room temperature for 1 h and filtered. Recrystallization from CH_2Cl_2 –hexane gave a yellow crystalline solid. Yield: 50 mg (83%). ^1H NMR (300 MHz, CDCl_3): δ = 1.73 (s, 15H, C_5Me_5), 2.63 (s, 2H, H_2O), 7.16 (dt, J_1 = 1.2 Hz, J_2 = 7.2 Hz, 1H, H^1), 7.23 (dt, J_1 = 1.2 Hz, J_2 = 7.2 Hz, 1H, H^2), 7.34 (dt, J_1 = 1.2 Hz, J_2 = 5.4 Hz, 1H, H^7), 7.65 (d, J = 1.2 Hz, 1H, H^3), 7.72 (d, J = 2.4 Hz, 1H, H^6), 7.80 (d, J = 1.2 Hz, 1H, H^4), 7.86 (d, J = 2.4 Hz, 1H, H^5), 8.95 (dt, J_1 = 1.2 Hz, J_2 = 5.4 Hz, 1H, H^8) ppm. $^{19}\text{F}\{^1\text{H}\}$ NMR (CDCl_3): δ = –77.8 ppm. Anal. Calc. for $\text{C}_{22}\text{H}_{25}\text{O}_4\text{NF}_3\text{Si}$: C, 40.73; H, 3.88; N, 2.16. Found: C, 41.12; H, 3.91; N, 2.11%.

2.3. Preparation of $[\text{Cp}^*\text{Ir}(\text{ppy})(\text{MeCN})][\text{OTf}]$ (**2**)

To a suspension of $[\text{Cp}^*\text{Ir}(\text{ppy})\text{Cl}]$ (50 mg, 0.096 mmol) in MeCN (10 mL) was added AgOTf (25 mg, 0.097 mmol). The mixture was stirred for 1 h and filtered. Recrystallization from MeCN–Et₂O gave yellow crystals which were suitable for X-ray diffraction analysis. Yield: 56 mg (87%). Alternatively, complex **2** could be obtained in good yield by recrystallization of complex **1** from MeCN–Et₂O. ^1H NMR (300 MHz, CDCl_3): δ = 1.73 (s, 15H, C_5Me_5), 2.41 (s, 3H, NCMe), 7.18 (dt, J_1 = 1.2 Hz, J_2 = 7.2 Hz, 1H, H^1), 7.26 (dt, J_1 = 1.2 Hz, J_2 = 7.2 Hz, 1H, H^2), 7.39 (dt, J_1 = 1.2 Hz, J_2 = 5.4 Hz, 1H, H^7), 7.68 (d, J = 1.2 Hz, 1H, H^3), 7.78 (d, J = 2.4 Hz, 1H, H^6), 7.85 (d, J = 1.2 Hz, 1H, H^4), 7.87 (d, J = 2.4 Hz, 1H, H^5), 8.93 (dt, J_1 = 1.2 Hz, J_2 = 5.4 Hz, 1H, H^8) ppm. $^{19}\text{F}\{^1\text{H}\}$ NMR (CDCl_3): δ = –77.8 ppm. Anal. Calc. for $\text{C}_{24}\text{H}_{26}\text{O}_3\text{N}_2\text{F}_3\text{Si}$: C, 42.91; H, 3.90; N, 4.17. Found: C, 42.88; H, 3.91; N, 4.11%.

2.4. Ir-catalyzed oxidation of styrene with PhIO

To a suspension solution of PhIO (220 mg, 1 mmol) and styrene (460 μL , 4 mmol) in CH_2Cl_2 (2.5 mL) at 0 °C was added complex **1** (0.01 mmol) in CH_2Cl_2 (2.5 mL). The mixture was stirred at 0 °C until all PhIO dissolved completely. The organic products were analyzed by GLC using an HP-1 column and quantified by internal standard method.

2.5. Ir-catalyzed aziridination of styrene with PhINTs

To a suspension solution of PhINTs (373 mg, 1 mmol) and styrene (460 μL , 4 mmol) in CH_2Cl_2 (2.5 mL) at 0 °C was added complex **1** (0.01 mmol) in CH_2Cl_2 (2.5 mL). The mixture was stirred at 0 °C until all PhINTs dissolved completely. The organic products were analyzed by GLC using an HP-1 column and quantified by internal standard method.

2.6. Preparation of $[\text{Cp}^*\text{Ir}(\eta^2\text{-ppy-NTs})(\text{MeCN})][\text{OTf}]$ (**3**)

To a solution of complex **2** (50 mg, 0.074 mmol) in dichloromethane (10 mL) at 0 °C was added PhINTs (27 mg, 0.075 mmol). The green mixture was slowly warmed to room temperature and stirred overnight to give a yellow solution. The volatiles were removed in vacuo and the residue was recrystallized from CH_2Cl_2 –hexane to give yellow crystals suitable for X-ray diffraction analysis. Yield: 48 mg (85%). ^1H NMR (300 MHz, CDCl_3): δ = 1.48 (s, 15H, C_5Me_5), 2.22 (s, 3H, $\text{C}_6\text{H}_4\text{CH}_3$), 2.44 (s, 3H, NCMe), 6.87 (d, J = 7.8 Hz, 2H, $\text{C}_6\text{H}_4\text{CH}_3$), 7.08 (m, 3H, $\text{C}_6\text{H}_4\text{CH}_3$ and H^1), 7.40 (m,

2H, H^2 and H^7), 7.77 (m, 2H, H^3 and H^6), 7.96 (d, J = 7.5 Hz, 1H, H^4), 8.11 (d, J = 8.4 Hz, 1H, H^5), 9.26 (d, J = 5.1 Hz, 1H, H^8) ppm. $^{19}\text{F}\{^1\text{H}\}$ NMR (CDCl_3): δ = –77.8 ppm. Anal. Calc. for $\text{C}_{31}\text{H}_{33}\text{N}_3\text{O}_5\text{F}_3\text{S}_2\text{Ir}$: C, 44.28; H, 3.96; N, 5.00. Found: C, 44.09; H, 3.93; N, 4.90%.

2.7. Preparation of $[\text{Cp}^*\text{Ir}(\text{ppy})(\eta^1\text{-E}_2\text{R}_2)][\text{OTf}]$ ($E = \text{S}$, $R = p\text{-tol}$) (**4**); $E = \text{Se}$, $R = \text{Ph}$ (**5**); $E = \text{Te}$, $R = \text{Ph}$ (**6**))

To a solution of complex **1** (50 mg, 0.074 mmol) in CH_2Cl_2 (10 mL) at 0 °C was added E_2R_2 (0.075 mmol). The resulting red mixture was stirred at room temperature overnight and a yellow solution was formed. The volatiles were removed in vacuo and the residue was recrystallized from CH_2Cl_2 –hexane to give yellow crystals which were suitable for X-ray diffraction analysis.

Complex 4: Yield: 54 mg (84%). ^1H NMR (300 MHz, CDCl_3): δ = 1.80 (s, 15H, C_5Me_5), 2.20 (s, 3H, $\text{C}_6\text{H}_4\text{CH}_3$), 2.26 (s, 3H, $\text{C}_6\text{H}_4\text{CH}_3$), 6.45 (d, J = 8.1 Hz, 2H, $\text{C}_6\text{H}_4\text{CH}_3$), 6.70 (d, J = 8.1 Hz, 2H, $\text{C}_6\text{H}_4\text{CH}_3$), 7.00 (d, J = 7.5 Hz, 2H, $\text{C}_6\text{H}_4\text{CH}_3$), 7.05 (d, J = 7.5 Hz, 2H, $\text{C}_6\text{H}_4\text{CH}_3$), 7.20–7.26 (m, 3H, H^1 , H^2 , H^7), 7.55 (d, J = 7.8 Hz, 2H, H^4 , H^5), 7.68 (t, J = 9.9 Hz, 2H, H^3 , H^6), 8.32 (s, 1H, H^8) ppm. $^{19}\text{F}\{^1\text{H}\}$ NMR (CDCl_3): δ = –77.6 ppm. Anal. Calc. for $\text{C}_{36}\text{H}_{37}\text{O}_3\text{N}_3\text{F}_3\text{S}_3\text{Ir}$: C, 49.30; H, 4.25; N, 1.60. Found: C, 49.35; H, 4.35; N, 1.79%.

Complex 5: Yield: 50 mg (78%). ^1H NMR (300 MHz, CDCl_3): δ = 1.84 (s, 15H, C_5Me_5), 6.40 (d, J = 8.1 Hz, 2H, Ph), 6.65 (d, J = 8.1 Hz, 2H, Ph), 7.05 (t, J = 7.5 Hz, 3H, Ph), 7.13 (t, J = 7.5 Hz, 3H, Ph), 7.22–7.29 (m, 3H, H^1 , H^2 , H^7), 7.62 (d, J = 7.8 Hz, 2H, H^4 , H^5), 7.74 (t, J = 9.9 Hz, 2H, H^3 , H^6), 8.45 (s, 1H, H^8) ppm. $^{19}\text{F}\{^1\text{H}\}$ NMR (CDCl_3): δ = –76.5 ppm. Anal. Calc. for $\text{C}_{34}\text{H}_{33}\text{O}_3\text{N}_3\text{F}_3\text{S}_2\text{Se}_2\text{Ir}$: C, 43.31; H, 3.53; N, 1.49. Found: C, 43.19; H, 3.60; N, 1.61%.

Complex 6: Yield: 54 mg, 73%. ^1H NMR (300 MHz, CDCl_3): δ = 1.78 (s, 15H, C_5Me_5), 6.42 (d, J = 8.1 Hz, 2H, Ph), 6.56 (d, J = 8.1 Hz, 2H, Ph), 6.89 (t, J = 7.5 Hz, 3H, Ph), 7.08 (t, J = 7.5 Hz, 3H, Ph), 7.18–7.26 (m, 3H, H^1 , H^2 , H^7), 7.54 (d, J = 7.8 Hz, 2H, H^4 , H^5), 7.68 (t, J = 9.9 Hz, 2H, H^3 , H^6), 8.36 (s, 1H, H^8) ppm. $^{19}\text{F}\{^1\text{H}\}$ NMR (CDCl_3): δ = –77.6 ppm. Anal. Calc. for $\text{C}_{34}\text{H}_{33}\text{O}_3\text{N}_3\text{F}_3\text{STe}_2\text{Ir}$: C, 39.26; H, 3.20; N, 1.35. Found: C, 40.17; H, 3.22; N, 1.37%.

2.8. Preparation of $[\text{Cp}^*\text{Ir}(\eta^2\text{-ppy-ER})(\text{H}_2\text{O})][\text{OTf}]_2$ ($E = \text{S}$, $R = p\text{-tol}$) (**7**); $E = \text{Se}$, $R = \text{Ph}$ (**8**))

To a solution of complex **4** or **5** (0.059 mmol) in CH_2Cl_2 (10 mL) was added AgOTf (26 mg, 0.10 mmol), the mixture was stirred at room temperature for 4 h. The volatiles were removed in vacuo and the residue was recrystallized from acetone–Et₂O to give yellow crystals which were suitable for X-ray diffraction analysis.

Complex 7: Yield: 35 mg (65%). ^1H NMR (300 MHz, acetone-*d*₆): δ = 1.56 (s, 15H, C_5Me_5), 2.20 (s, 3H, $\text{C}_6\text{H}_4\text{CH}_3$), 2.87 (s, 2H, H_2O), 6.98 (d, J = 8.1 Hz, 2H, $\text{C}_6\text{H}_4\text{CH}_3$), 7.05 (d, J = 8.1 Hz, 2H, $\text{C}_6\text{H}_4\text{CH}_3$), 7.59 (d, J = 17.1 Hz, 1H, H^1), 7.83 (t, J = 7.8 Hz, 2H, H^2 , H^7), 8.23–8.29 (m, 2H, H^3 , H^6), 8.43 (d, J = 5.4 Hz, 2H, H^4 , H^5), 9.03 (s, 1H, H^8) ppm. $^{19}\text{F}\{^1\text{H}\}$ NMR (CDCl_3): δ = –78.5 ppm. Anal. Calc. for $\text{C}_{30}\text{H}_{32}\text{O}_7\text{NF}_6\text{S}_3\text{Ir}$: C, 39.13; H, 3.50; N, 1.52. Found: C, 38.98; H, 3.54; N, 1.33%.

Complex 8: Yield: 32 mg (53%). ^1H NMR (300 MHz, acetone-*d*₆): δ = 1.54 (s, 15H, C_5Me_5), 3.12 (s, 2H, H_2O), 7.12 (d, J = 8.1 Hz, 2H, Ph), 7.27 (t, J = 8.1 Hz, 3H, Ph), 7.78 (d, J = 21.4 Hz, 1H, H^1), 8.10 (t, J = 8.2 Hz, 2H, H^2 , H^7), 8.18–8.29 (m, 2H, H^3 , H^6), 8.39 (d, J = 7.7 Hz, 2H, H^4 , H^5), 8.97 (s, 1H, H^8) ppm. $^{19}\text{F}\{^1\text{H}\}$ NMR (CDCl_3): δ = –78.5 ppm. Anal. Calc. for $\text{C}_{29}\text{H}_{30}\text{O}_7\text{NF}_6\text{S}_2\text{SeIr}$: C, 36.52; H, 3.17; N, 1.49. Found: C, 36.33; H, 3.14; N, 1.33%.

2.9. X-ray crystallography

Crystal data and experimental details for complexes **2–7** are summarized in Table 1. Preliminary examinations and intensity data collection were carried out on a Bruker SMART-APEX 1000

Table 1
Crystallographic data and experimental details for complexes 2–7.

	2	3	4	5	6	7
Formula	C ₂₄ H ₂₆ F ₃ IrN ₂ O ₃ S	C ₃₁ H ₃₃ F ₃ IrN ₃ O ₅ S ₂	C ₃₆ H ₃₇ F ₃ IrNO ₃ S ₃	C ₃₄ H ₃₃ F ₃ IrNO ₃ SSe ₂	C ₃₄ H ₃₃ F ₃ IrNO ₃ STe ₂	C ₃₀ H ₃₂ F ₆ IrNO ₇ S ₃
Formula weight	671.73	840.92	877.05	942.79	1040.07	920.95
a (Å)	12.129(8)	15.734(2)	12.2352(10)	11.5234(7)	11.3662(6)	16.5553(14)
b (Å)	13.151(9)	14.689(2)	15.5541(13)	15.2084(9)	15.6741(9)	12.3006(11)
c (Å)	15.612(1)	14.266(2)	19.1033(16)	19.5704(11)	19.7157(11)	32.598(3)
α (°)	90	90	90	90	90	90
β (°)	102.519(1)	95.342(2)	104.838(2)	101.877(1)	101.891(1)	90
γ (°)	90	90	90	90	90	90
V (Å ³)	2431.1(3)	3282.8(7)	3514.3(5)	3356.3(3)	3437.1(3)	6638.2(10)
Z	4	4	4	4	4	8
Crystal system	Monoclinic	Monoclinic	Monoclinic	Monoclinic	Monoclinic	Orthorhombic
Space group	P2 ₁ /c	P2 ₁ /c	P2 ₁ /c	P2 ₁ /c	P2 ₁ /c	Pbca
ρ _{calc} (g cm ⁻³)	1.835	1.701	1.658	1.866	2.010	1.843
T (K)	100(2)	298(2)	173(2)	173(2)	173(2)	173(2)
μ (mm ⁻¹)	5.630	4.255	4.030	6.261	5.660	4.292
F(0 0 0)	1312	1664	1744	1824	1968	3632
Number of reflections	12 554	23 116	18 155	22 959	16 365	37 897
Number of independent reflections	4188	5734	5600	5826	5498	5578
R _{int}	0.0480	0.0877	0.0599	0.0242	0.0559	0.1012
R1, wR2 (I > 2σ(I))	0.0418, 0.0759	0.0556, 0.0774	0.0492, 0.0894	0.0210, 0.0493	0.0644, 0.1244	0.0335, 0.0494
R1, wR2 (all data)	0.0539, 0.0792	0.1000, 0.0842	0.0705, 0.0959	0.0267, 0.0508	0.0835, 0.1320	0.0746, 0.0541
GOF	1.080	0.975	1.013	1.034	1.034	0.964

area-detector diffractometer using graphite-monochromated Mo K α radiation ($\lambda = 0.70173$ Å). The collected frames were processed with the software SAINT and the data was corrected for absorption using the program SADABS [15]. Structures were solved by direct methods and refined by full-matrix least-squares on F^2 using the SHELXTL software package [16]. Unless stated otherwise, non-hydrogen atoms were refined with anisotropic displacement parameters. Carbon-bonded hydrogen atoms were included in calculated positions and refined in the riding mode using SHELXL97 default parameters.

3. Results and discussion

3.1. Reaction of [Cp*Ir(ppy)(solv)]⁺ with oxo donors

Treatment of [Cp*Ir(ppy)Cl] with Ag(OTf) (OTf⁻ = triflate) in MeOH and MeCN gave the solvento complexes [Cp*Ir(ppy)(solv)]

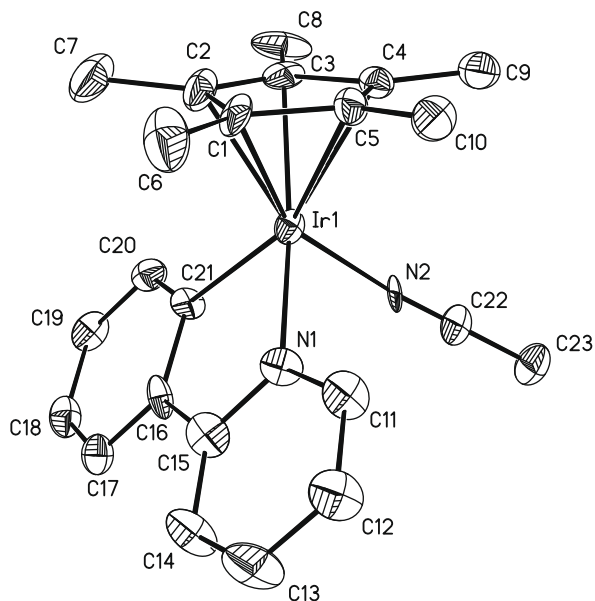


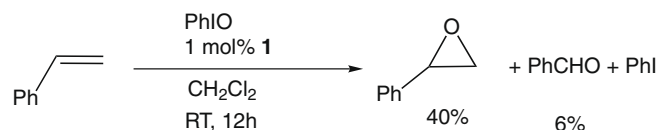
Fig. 1. Molecular structure of the complex cation in **2**. Hydrogen atoms are omitted for clarity. The ellipsoids are drawn at a 50% probability level.

Table 2
Selected bond lengths (Å) and angles (°) for [Cp*Ir(ppy)(MeCN)]⁺ [OTf]⁻ (**2**).

Ir(1)–N(1)	2.103(5)	Ir(1)–N(2)	2.039(5)
Ir(1)–C(1)	2.144(6)	Ir(1)–C(2)	2.159(7)
Ir(1)–C(3)	2.153(7)	Ir(1)–C(4)	2.225(6)
Ir(1)–C(5)	2.237(6)	Ir(1)–C(21)	2.047(6)
C(22)–N(2)–Ir(1)	173.2(5)	N(2)–Ir(1)–N(1)	86.0(2)
C(21)–Ir(1)–N(1)	78.3(2)	N(2)–Ir(1)–C(21)	89.2(2)

[OTf] (solv = H₂O (**1**), MeCN (**2**)). Complex **2** also could be prepared by recrystallization of **1** from MeCN–Et₂O. Fig. 1 shows the structure of the complex cation in **2**; selected bond lengths and angles are listed in Table 2. The Ir–C(Cp*) (av. 2.184(7) Å), Ir–C(ppy) (2.047(6) Å), and Ir–N(ppy) (2.103(5) Å) distances are similar to those in [Cp*Ir(ppy)Cl] [9]. The Ir–NCMe distance of 2.039(5) Å compares well with that of [Cp*Ir(PPh₃)(NCMe)₂]⁺ (2.086(8) and 2.066(8) Å) [17].

In an attempt to synthesize Ir-oxo species, reactions of **1** with oxo donors have been investigated. Addition of 1 equivalent of PhIO to **1** in CH₂Cl₂ at –10 °C resulted in dissolution of PhIO and formation reactive green species and PhI. The green species was thermally unstable and decomposed to **1** above 0 °C. Despite many attempts, we have not been able to isolate or characterize this green species. The decomposition of PhIO was found to be catalytic with respect to Ir. For example, treatment of PhIO with 1 mol% of **1** afforded PhI in 56% yield. In the presence of excess styrene, this reaction afforded a ca. 7:1 mixture of styrene oxide and benzaldehyde with a total turnover number (TON) of 46 (Scheme 2), suggesting that the green species is possibly an Ir-oxo species that can transfer the oxo group to styrene. An alternative candidate of the green species is an Ir–I(O)Ph adduct [18], in which the Ir^{III} = O group is activated by the Lewis acidic Ir center. Complex **1** can also catalyze the oxidation of styrene with *tert*-butylhydroperoxide,



Scheme 2. Ir-catalyzed oxidation of styrene with PhIO.

albeit with a smaller TON (16) and lower selectivity (styrene oxide/benzaldehyde ratio of ca. 1.5:1). Additional studies are required to elucidate the mechanism of the Ir-catalyzed epoxidation.

3.2. Reaction of $[\text{Cp}^*\text{Ir}(\text{ppy})(\text{solv})]^+$ with PhINTs

We next turned our attention to the reaction of **1** with nitrene donors. Treatment of **1** with PhINTs at -10°C resulted in a green solution that turned yellow upon warming to ca. 0°C . We have not been able to trap or characterize the green or yellow species. Nevertheless, for the reaction of **2** with PhINTs afforded, a yellow crystalline product characterized as the ppy-tosylamido complex $[\text{Cp}^*\text{Ir}(\eta^2\text{-ppy-NTs})(\text{MeCN})][\text{OTf}]$ (**3**) was isolated (Scheme 3). The presence of the tosyl group in **3** was evidenced by ^1H NMR ($\delta = 2.22$ ppm) and IR (1063 cm^{-1} , $\nu(\text{S}=\text{O})$) spectroscopies. Treatment of PhINTs with styrene in the presence of 1 mol% of **1** afforded styrene tosylaziridine with a TON of 15 (Scheme 4), suggesting that the green intermediate (possibly an Ir-nitrene species) can act as a nitrene transfer agent. Compound **3** could also be synthesized by reaction of **2** with TsN_3 that is a typical nitrene precursor, lending further support for the nitrene transfer from PhINTs to Ir. A possible mechanism for the formation of compound **3** is shown in Scheme 3. Reaction of PhINTs with **1** initially gives a transient Ir=NTs species, possibly $[\text{Cp}^*\text{Ir}(\text{ppy})(\text{NTs})]^+$, that transfers the NTs group to styrene. In the absence of olefin, the nitrene group inserts into the Ir–C(ppy) bond to yield **3**. It should be noted that insertion of nitrene group into the Pd–C bond of a palladacycle has been reported recently. A stepwise mechanism involving a Pd^{IV} nitrene intermediate and migratory insertion of the nitrene group into the Pd–C bond has been proposed [19].

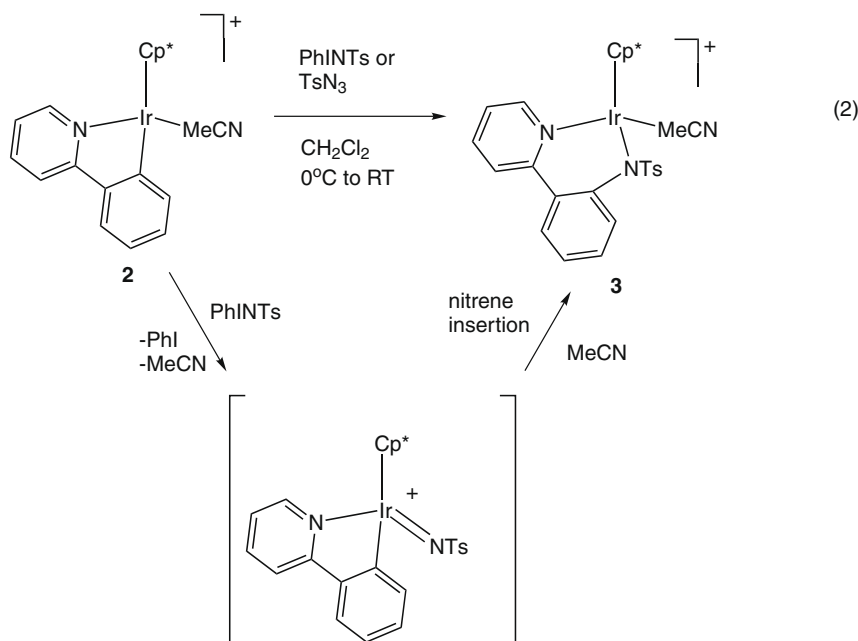
The molecular structure of the cation $[\text{Cp}^*\text{Ir}(\eta^2\text{-ppy-NTs})(\text{MeCN})]^+$ in **3** is shown in Fig. 2; selected bond lengths and angles are listed in Table 3. The Ir–C(Cp^{*}) and Ir–N(ppy) distances (2.158(9) and 2.133(6) Å, respectively) are similar to those in **2**. The ppy moiety is twisted with the dihedral angle between the pyridyl and phenyl rings of 37.1° apparently due to insertion of the NTs group. The Ir–N(amide) distance of 2.112(6) Å is similar to that in $[\text{Cp}^*\text{Ir}(\text{PMe}_3)\text{Ph}(\text{NH}_2)]$ (2.105(8) Å) [20].

3.3. Reaction of $[\text{Cp}^*\text{Ir}(\text{ppy})(\text{solv})]^+$ with R_2E_2

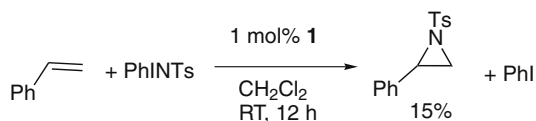
Oxidative addition of R_2E_2 (E = S or Se) is a convenient synthetic route of transition metal thiolate complexes. Of particular interest are Pd^{IV} and Pt^{IV} bis(chalcogenolate) complexes, which are involved in metal-catalyzed selective addition of E–E bonds to alkynes [21]. Recently, we reported that reaction of Ir^{III} alkyl complexes with R_2S_2 led to formation of Ir^{III} bis(thiolate) complexes, possibly via oxidative addition of the S–S bond to Ir^{III} and subsequent C–S bond elimination [22]. Thus, in an attempt to prepare higher valent Cp^*Ir chalcogenolate complexes, reactions of **1** with R_2E_2 (E = S, Se, Te) were attempted. However, instead of oxidative addition of the E–E bond, reaction of **1** with R_2E_2 led to isolation of the Ir^{III} η^1 -dichalcogenide complexes $[\text{Cp}^*\text{Ir}(\text{ppy})(\eta^1\text{-E}_2\text{R}_2)][\text{OTf}]$ (E = S, R = *p*-tol (**4**); E = Se, R = Ph (**5**); E = Te, R = Ph (**6**)) (Scheme 5). The ^1H NMR spectrum of **4** displayed two singlets at δ 2.20 and 2.26 ppm due to the *p*-Me protons of the tolyl groups, consistent with the η^1 -binding mode of the disulfide ligand. It should be noted that R_2E_2 usually binds to metal in a $\mu\text{-}\eta^1, \eta^1$ fashion, e.g. $[\text{CpMn}(\text{CO})_2]_2(\mu\text{-RE-ER})$ [23]. Metal complexes containing $\eta^1\text{-RE-ER}$ ligands, which have been suggested to be an intermediate in oxidative addition of R_2E_2 with $\text{Pd}(0)$, are less common [24].

The crystal structures of the complex cations in **4–6** are shown in Figs. 3–5, respectively; selected bond lengths and angles are compiled in Table 4. The Ir–C(Cp^{*}), Ir–C(ppy) (2.053(7), 2.052(2) and 2.053(12) Å, respectively), and Ir–N(ppy) (2.095(6), 2.087(2) and 2.087(10) Å, respectively) distances for **4–6** are similar to those of **2**. The corresponding Ir–E (2.335(18), 2.451(3) and 2.593(9) Å) and E–E (2.091(3), 2.370(5) and 2.593(9) Å) distances are consistent with the trend of covalent radii of the chalcogens.

Interestingly, treatment of **4** and **5** with excess $\text{Ag}(\text{OTf})$ led to cleavage of the E–E bond. Migratory insertion of one of the ER groups into the Ir–C(ppy) bond afforded the η^2 -pyridyl-chalcogenolate complexes $[\text{Cp}^*\text{Ir}\{\eta^2\text{-ppy-ER}(\text{H}_2\text{O})\}][\text{OTf}]_2$ (E = S, R = *p*-tolyl (**7**); E = Se, R = Ph (**8**)) (Scheme 5). The fate of the remaining ER group has not been studied. The ^1H NMR spectrum of **7** shows only one methyl resonance signal at $\delta = 2.20$ ppm, indicating that the loss of one *p*-tolS group in the disulfide ligand. In addition, a singlet at $\delta = 3.12$ ppm assignable to the H_2O ligand was observed.



Scheme 3. Synthesis of complex **3**.



Scheme 4. Ir-catalyzed aziridination of styrene with PhINTs.

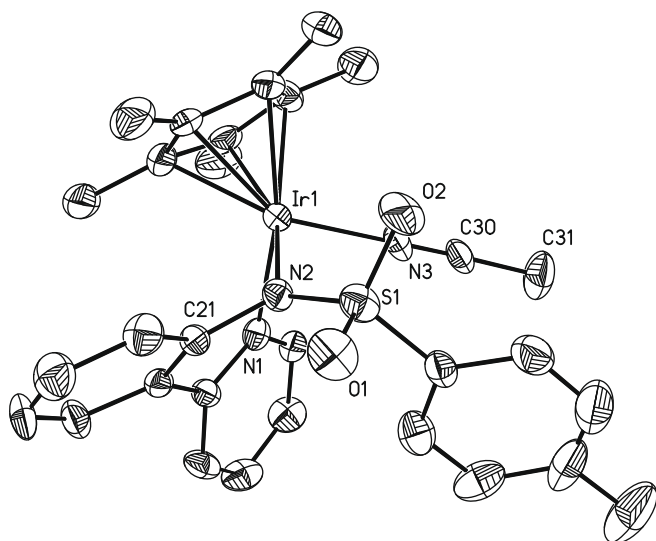


Fig. 2. Molecular structure of the complex cation in **3**. Hydrogen atoms are omitted for clarity. The ellipsoids are drawn at a 50% probability level.

Table 3
Selected bond lengths (Å) and angles (°) for [Cp*Ir(η²-ppy-NTs)(MeCN)][OTf] (**3**).

Ir(1)–N(1)	2.133(6)	Ir(1)–N(2)	2.112(6)
Ir(1)–N(3)	2.025(8)	Ir(1)–C(1)	2.167(8)
Ir(1)–C(2)	2.149(9)	Ir(1)–C(3)	2.163(9)
Ir(1)–C(4)	2.177(9)	Ir(1)–C(5)	2.136(8)
N(2)–Ir(1)–N(1)	80.5(2)	N(3)–Ir(1)–N(1)	84.4(2)
N(3)–Ir(1)–N(2)	91.2(3)	C(21)–N(2)–Ir(1)	113.2(5)
S(1)–N(2)–Ir(1)	125.7(4)	C(30)–N(3)–Ir(1)	171.8(8)

The molecular structure of the complex cation in **7** is shown in Fig. 6; selected bond lengths and angles are listed in Table 5. The Ir–C(Cp*) (av. 2.170(5) Å) and Ir–S (2.3639(12) Å) distances for **7** are similar to those in **4**. However, the Ir–N(ppy) (2.127(4)) Å distance is longer than that in **4**, presumably due to the formation of the six-membered metallacycle. The torsion angle between the

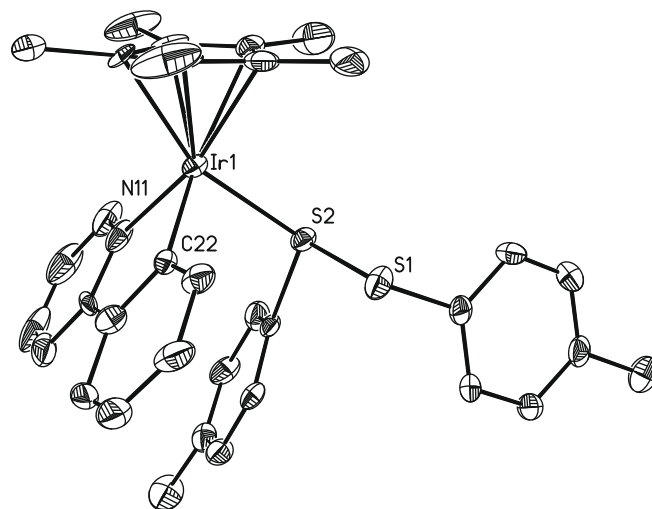


Fig. 3. Molecular structure of the complex cation in **4**. Hydrogen atoms are omitted for clarity. The ellipsoids are drawn at a 50% probability level.

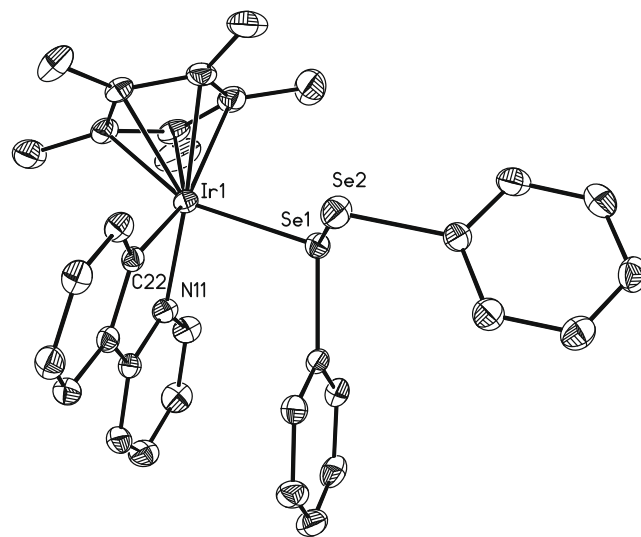
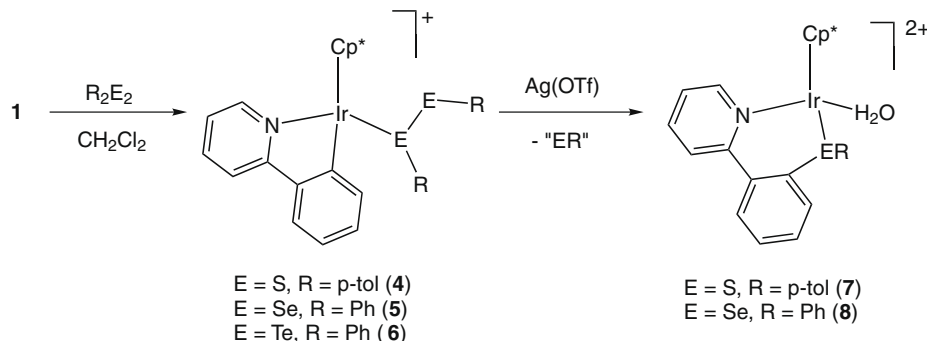


Fig. 4. Molecular structure of the complex cation in **5**. Hydrogen atoms are omitted for clarity. The ellipsoids are drawn at a 50% probability level.

pyridine and phenyl rings in the ppy moiety is determined to be 43.5°.



Scheme 5. Synthesis of complexes **4–8**.

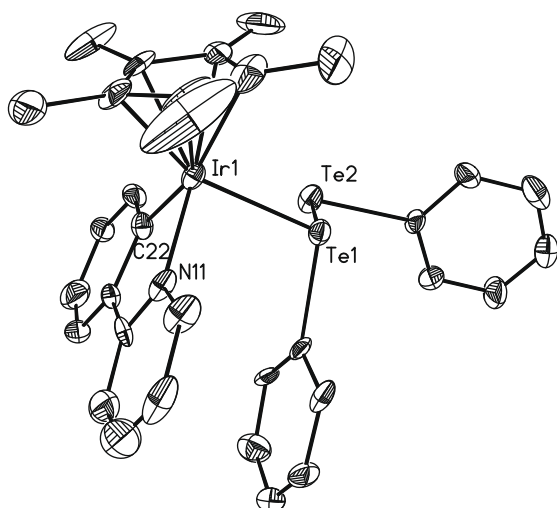


Fig. 5. Molecular structure of the complex cation in **6**. Hydrogen atoms are omitted for clarity. The ellipsoids are drawn at a 50% probability level.

Table 4

Selected bond lengths (Å) and angles (°) for $[\text{Cp}^*\text{Ir}(\text{ppy})(\eta^1\text{-R}_2\text{E}_2)]\text{[OTf]}$ (RE = *p*-tolS, PhSe, PhTe).

	RE = <i>p</i> -tolS (4)	RE = PhSe (5)	RE = PhTe (6)
Ir–Cp*	2.168(8)	2.173(3)	2.157(12)
	2.173(6)	2.183(3)	2.192(11)
	2.189(7)	2.204(3)	2.212(13)
	2.245(7)	2.260(3)	2.220(16)
	2.263(8)	2.261(3)	2.225(14)
Ir–C(ppy)	2.053(7)	2.052(3)	2.053(12)
Ir–N	2.095(6)	2.087(2)	2.087(10)
Ir–E	2.3350(18)	2.4508(3)	2.5930(9)
C(ppy)–Ir(1)–E	89.60(19)	89.63(8)	77.5(5)
C(ppy)–Ir(1)–N	77.9(3)	78.00(10)	89.4(3)
E–Ir(1)–N	90.13(7)	89.67(7)	89.5(3)
Ir–E–E'	109.44(9)	106.120(16)	102.56(3)
Ir–E–C(RE)	111.0(2)	108.34(9)	105.0(3)

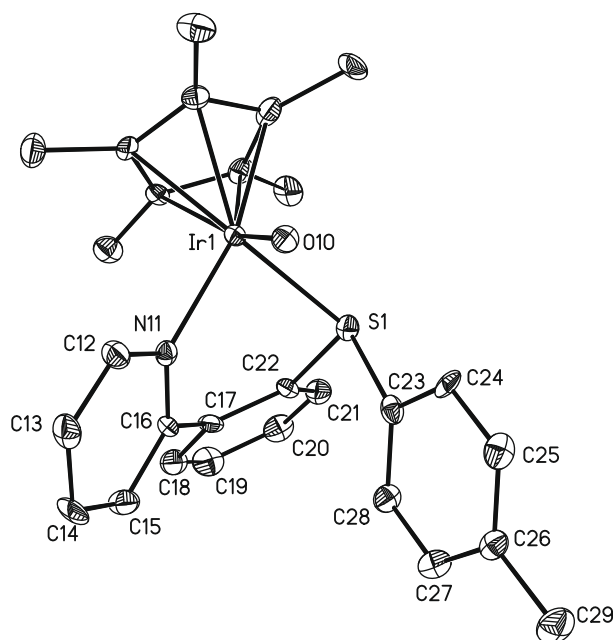


Fig. 6. Structure of the complex cation in **7**. Hydrogen atoms are omitted for clarity. The ellipsoids are drawn at a 50% probability level.

Table 5

Selected bond lengths (Å) and angles (°) for $[\text{Cp}^*\text{Ir}(\eta^2\text{-ppy-Stol})(\text{H}_2\text{O})]\text{[OTf]}_2$ (**7**).

Ir(1)–N(11)	2.127(4)	Ir(1)–O(10)	2.153(3)
Ir(1)–S(1)	2.3639(12)	Ir(1)–C(1)	2.181(5)
Ir(1)–C(2)	2.141(5)	Ir(1)–C(3)	2.175(5)
Ir(1)–C(4)	2.179(5)	Ir(1)–C(5)	2.172(6)
N(11)–Ir(1)–O(10)	83.23(13)	C(22)–S(1)–Ir(1)	98.49(17)
N(11)–Ir(1)–S(1)	85.77(12)	C(23)–S(1)–Ir(1)	118.35(17)
O(10)–Ir(1)–S(1)	89.51(9)		

4. Conclusions

In summary, we have studied the reactions of $[\text{Cp}^*\text{Ir}(\text{ppy})(\text{H}_2\text{O})]^+$ with oxo and nitrene donors. We found that $[\text{Cp}^*\text{Ir}(\text{ppy})(\text{H}_2\text{O})]^+$ can catalyze the epoxidation of styrene with PhIO, possibly via a high-valent Ir-oxo active species. Reaction of $[\text{Cp}^*\text{Ir}(\text{ppy})(\text{MeCN})]^+$ with PhINTs led to migratory insertion of the nitrene into the Ir–C(ppy) bond and formation of $[\text{Cp}^*\text{Ir}(\eta^2\text{-ppy-NTs})(\text{MeCN})]^+$. Reaction of $[\text{Cp}^*\text{Ir}(\text{ppy})(\text{H}_2\text{O})]^+$ with R_2E_2 led to the formation of the adducts $[\text{Cp}^*\text{Ir}(\text{ppy})(\eta^1\text{-E}_2\text{R}_2)]^+$ that reacted with $\text{Ag}(\text{OTf})$ to give $[\text{Cp}^*\text{Ir}(\eta^2\text{-ppy-ER})(\text{H}_2\text{O})]^{2+}$.

5. Supplementary material

CCDC 609384, 609385 and 619389–609392 contain the supplementary crystallographic data complexes **2–7**. These data can be obtained free of charge from The Cambridge Crystallographic Data Centre via www.ccdc.cam.ac.uk/data_request/cif.

Acknowledgment

We thank Dr. Herman H.Y. Sung for solving the crystal structures. The financial support from the Hong Kong Research Grants Council (Project No. 601708) is gratefully acknowledged.

References

- [1] A.H. Janowicz, R.G. Bergman, *J. Am. Chem. Soc.* 104 (1982) 352–354.
- [2] J.K. Hoyano, W.A.G. Graham, *J. Am. Chem. Soc.* 104 (1982) 3723–3725.
- [3] B.A. Arndsten, R.G. Bergman, T.A. Mobley, T.H. Peterson, *Acc. Chem. Res.* 28 (1995) 154–162.
- [4] B.A. Arndtsen, R.G. Bergman, *Science* 270 (1995) 1970–1973.
- [5] D.L. Strout, S. Zarić, S. Niu, M.B. Hall, *J. Am. Chem. Soc.* 118 (1996) 6068–6069.
- [6] M.-D. Su, S.-Y. Chu, *J. Am. Chem. Soc.* 119 (1997) 5373–5383.
- [7] S.R. Klei, T.D. Tilley, R.G. Bergman, *J. Am. Chem. Soc.* 122 (2000) 1816–1817.
- [8] N.D. McDaniel, F.J. Coughlin, L.L. Tinker, S. Bernhard, *J. Am. Chem. Soc.* 130 (2008) 210–217.
- [9] J.F. Hull, D. Balcells, J.D. Blakemore, C.D. Incavito, O. Eisenstein, G.W. Brudvig, R.H. Crabtree, *J. Am. Chem. Soc.* 131 (2009) 8730–8731.
- [10] R.S. Hay-Motherwell, G. Wilkinson, B. Hussain-Bates, M.B. Hursthouse, *Polyhedron* 12 (1993) 2009–2012.
- [11] D.S. Glueck, J. Wu, F.J. Hollander, R.G. Bergman, *J. Am. Chem. Soc.* 113 (1991) 2041–2054.
- [12] W.D. McGhee, T. Foo, F.J. Hollander, R.G. Bergman, *J. Am. Chem. Soc.* 110 (1988) 8543–8545.
- [13] D.A. Dobbs, R.G. Bergman, *Organometallics* 13 (1994) 4594–4605.
- [14] D.L. Davies, O. Al-Duaij, J. Fawcett, M. Giardiello, S.T. Hilton, D.R. Russell, *Dalton Trans.* (2003) 4132–4138.
- [15] SMART and SAINT+ for Windows NT V6.02a, Bruker Analytical X-ray Instruments Inc., Madison, Wisconsin, USA, 1998.
- [16] G.M. Sheldrick, *SHELXTL-PLUS V5.1 Software Reference Manual*, Bruker AXS Inc., Madison, Wisconsin, USA, 1997.
- [17] F. Hanasaka, K.I. Fujita, R. Yamaguchi, *Organometallics* 24 (2005) 3422–3433.
- [18] J.P. Collman, A.S. Chien, T.A. Eberspacher, J.I. Brauman, *J. Am. Chem. Soc.* 122 (2000) 11098–11100.
- [19] A.R. Dick, M.S. Remy, J.W. Kampf, M.S. Sanford, *Organometallics* 26 (2007) 1365–1370.
- [20] D. Rais, R.G. Bergman, *Chem.–Eur. J.* 10 (2004) 3970–3978.
- [21] I. Beletskaya, C. Moberg, *Chem. Rev.* 99 (1999) 3435–3462.
- [22] Q.-F. Zhang, K.-M. Cheung, H.S.Y. Sung, I.D. Williams, W.-H. Leung, *Eur. J. Inorg. Chem.* (2005) 4780–4787.
- [23] J.M. Gonzales, D.G. Musaev, K. Morokuma, *Organometallics* 24 (2005) 4908–4914.
- [24] R.D. Adams, J.W. Long, J.L. Perrin, *J. Am. Chem. Soc.* 120 (1998) 1922–1923.